BiCMOS Current-Controlled Current Feedback Amplifier (CC-CFA) and Its Applications

MONTREE SIRIPRUCHYANUN[1], CHAIYAN CHANAPROMMA[2], PHAMORN SILAPAN[3] and WINAI JAIKLA[4]

[1,2] Department of Teacher Training in Electrical Engineering, Faculty of Technical Education, King Mongkut's University of Technology North Bangkok, Bangkok, 10800, THAILAND
[3] Electric and Industrial Program, Faculty of Industrial Technology, Uttaradit Rajabhat University, Muang, Uttaradit, 53000, THAILAND
[4] Electric and Electronic Program, Faculty of Industrial Technology, Suan Sunandha Rajabhat University, Dusit, Bangkok, 10300, THAILAND
mts@kmutnb.ac.th, chaiyanc@kmutnb.ac.th, phamorn@mail.uru.ac.th, jnai2004@yahoo.com
http://www.te.kmutnb.ac.th/~msn/

Abstract: - This paper introduces a modified version of current feedback amplifier (CFA), called current controlled current feedback amplifier (CC-CFA), to extend usabilities of this active element in terms of electronic control-abilities and simpler circuit description of the element's applications. This modified element was realized by using a BiCMOS standard technology to reduce offset error phenomenon, the design configuration is systematically explained. The performances have been proven through PSPICE which is accordance with theoretical anticipations. In addition, application examples for a current-mode multiplier/divider, oscillator, grounded inductance simulator, filters, and amplifiers are included. The results are confirmed that the electrical characteristics are electronically tunable.

Key-Words: - CC-CFA, Current-mode, Voltage-mode, Filter, Oscillator, Inductance simulator, Multiplier

1 Introduction

There has been much effort to reduce the supply voltage of electronic circuits in the last decade. This is due to the demand for portable and battery-powered equipment. Since a low-voltage operating circuit becomes necessary, the current-mode technique is ideally suited for this purpose more than the voltage-mode one. Consequently, there is a growing interest in synthesizing the current-mode circuits because of more their potential advantages such as larger dynamic range, higher signal bandwidth, greater linearity, simpler circuitry and low power consumption [1-2]. Many active elements able to function in current-mode such as OTA, current feedback amplifier, current conveyor [3], current differencing buffered amplifier (CDBA) [4] and current differencing transconductance amplifier (CDTA) [5], and etc., have been introduced to response these demands.

Among the mentioned active building blocks, the current feedback amplifier (CFA) or current feedback operational amplifier (CFOA) is an interesting active component, especially suitable for a class of analog signal processing [6-8]. This device can operate in both current and voltage-modes, provides flexibility and enables a variety of circuit designs. In addition, it can offer advantageous features such as high-slew rate, free from parasitic capacitances, wide bandwidth and simple implementation [9-11], Presently, the CFA can be commercially found, for example AD844 of Analog Devices Inc. [7]. It can be employed to realize filters [10-13], amplifiers [14], oscillators [15-19], inductance simulators [20-21], and etc. [22-24]. Conventionally, the electrical characteristics for applications of the CFAs cannot be adjusted by electronic methods, which this means that they cannot be controlled by currents and/or voltages. Although, they can be achieved by passive element adjustments, the electronic control method is being more popular more than those by passive elements (i.e. resistors and capacitors) [25] due to it can be easily adapted to automatic or microcontroller-based controls [26]. In addition, the CFA can not be controlled by the parasitic resistance at current input port so when it is used in a circuit, it must unavoidably require some external passive components, especially the resistors. This makes it not appropriate for IC implementation due to occupying more chip area, high power dissipation and cannot be electronic controllable. If it is employed for an off-the-shelf design, the circuit

description is composed of a large number of external passive elements. Actually, the electronic control can be done in a CFA application by replacing a resistor by junction field effect transistor (JFET) employed in voltage controlled resistor (VCR) region [19]. Unfortunately, it makes circuit description more complicated. Furthermore, the conventional CFA was designed by using the BJT and a basic voltage follower, consequently, this structure has problem for the output offset errors because the BJT current mirrors in the CFA provide errors due to practically internal factors more than a current mirror based on CMOS [27]. The offset output error from the basic voltage follower also affects the accuracies of circuits/systems. The offset problem is an important factor for circuit designers to be certain in practical implementations, especially in instrumentation and measurement systems.

In this work, thus, a modified-version CFA whose parasitic resistance at current input port can be controlled by an input bias current, called current controlled current feedback amplifier (CC-CFA), will be reviewed via this article. To reduce offset phenomenon, a BiCMOS technology is suitable for realizing the proposed element. In addition, the voltage follower is also developed to reduce the offset output current and voltage. The performances of proposed BiCMOS CC-CFA are illustrated by PSPICE simulations, they show good agreement as mentioned. The example applications as a multiplier/divider, oscillator, grounded inductance simulator, filters, and amplifiers are included.

2 Circuit Configuration

2.1 Basic Concept of CFA

The CFA properties can be shown in the following equation

$$\begin{bmatrix} I_y \\ V_x \\ I_z \\ V_w \end{bmatrix} = \begin{bmatrix} 0 & 0 & 0 & 0 \\ 0 & 1 & 0 & 0 \\ 1 & 0 & 0 & 0 \\ 0 & 0 & 1 & 0 \end{bmatrix} \begin{bmatrix} I_x \\ V_y \\ V_z \\ V_w \end{bmatrix}. \quad (1)$$

The symbol and the equivalent circuit of the CFA are illustrated in Fig. 1(a) and (b), respectively. A circuit implementation of CFA can be achieved by using second-generation current conveyor (CCII) as input stage, followed by a buffered amplifier as depicted in Fig. 1(c).

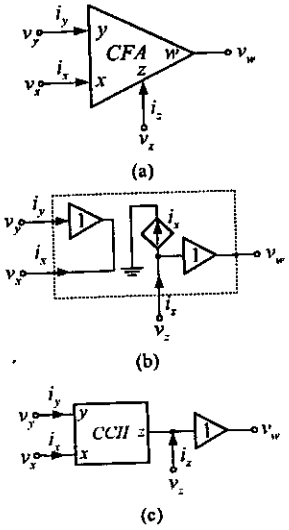

Figure 1. CFA (a) Symbol (b) Equivalent circuit (Element implementation

2.2 Basic Concept of CC-CFA

CC-CFA properties are similar to the conventio CFA, except that the CC-CFA has finite in resistance R_x at the x input terminal. This parasi resistance can be controlled by the bias current I_B shown in the following equation

$$\begin{bmatrix} I_y \\ V_x \\ I_z \\ V_w \end{bmatrix} = \begin{bmatrix} 0 & 0 & 0 & 0 \\ R_x & 1 & 0 & 0 \\ 1 & 0 & 0 & 0 \\ 0 & 0 & 1 & 0 \end{bmatrix} \begin{bmatrix} I_x \\ V_y \\ V_z \\ V_w \end{bmatrix},$$

where

$$R_x = \frac{V_T}{2I_B}.$$

V_T is the thermal voltage, which is 26mV at r temperature. The symbol and equivalent circui the CC-CFA are illustrated in Fig. 2(a) and respectively. In similar, we can realize the CC-C by using second-generation current contro current conveyor (CCCII) as input stage, follo by a buffered amplifier as illustrated in Fig. 2(c).

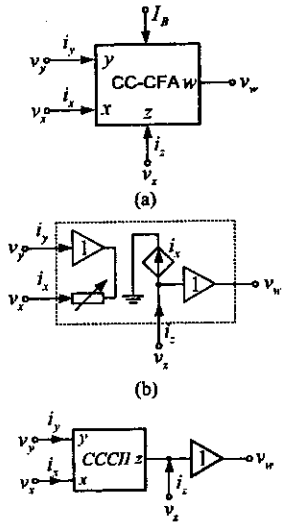

Figure 2. CC-CFA (a) Symbol (b) Equivalent circuit (c) Element implementation

2.3 Simple BJT current mirror compared to MOS current mirror

Since the current mirror is the basic block to realize CC-CFA, a comparison of the simple BJT and MOS current mirrors will be shown in this section. Fig. 3(a) displays the BJT current mirror. From routine analysis, the output current can be expressed to be [27]

$$I_{out} = \frac{\frac{I_{S2}}{I_{S1}} I_{in}\left(1+\frac{V_{CE2}-V_{CE1}}{V_A}\right)}{1+\frac{1-(I_{S2}/I_{S1})}{\beta_F}}. \quad (4)$$

If I_{S2}/I_{S1} is the ideal gain of the BJT current mirror and V_A is the Early voltage, the systematic gain error of the BJT current mirror (ε_{BJT}) can be found to be

$$\varepsilon_{BJT} = \frac{\left(1+\frac{V_{CE2}-V_{CE1}}{V_A}\right)}{1+\frac{1-(I_{S2}/I_{S1})}{\beta_F}} \cong \frac{V_{CE2}-V_{CE1}}{V_A} - \frac{1-(I_{S2}/I_{S1})}{\beta_F}. \quad (5)$$

From Eq. (5), the first term is originated from finite output resistance and the second term comes from finite β_F. The MOS current mirror is illustrated in Fig. 3(b). By straightforward analysis, we will receive

$$I_{out} = \frac{(W/L)_2}{(W/L)_1} I_{in}\left(1+\frac{V_{DS2}-V_{DS1}}{V_A}\right). \quad (6)$$

If $(W/L)_2/(W/L)_1$ is the ideal gain of the MOS current mirror, the systematic gain error of the MOS current mirror (ε_{MOS}) can be expressed to be

$$\varepsilon_{MOS} = \frac{V_{DS2}-V_{DS1}}{V_A}. \quad (7)$$

From Eq. (7), the gain error of the MOS current mirror stems from only the finite output resistance implied from the Early voltage which differs from the gain error of the BJT as depicted in Eq. (5). This result shows that the MOS current mirror has more accuracy than the BJT one. One reason is that the MOS generally provides higher Early voltage than the BJT does [27]. Consequently, CMOS is employed in the current mirrors to implement the proposed CC-CFA.

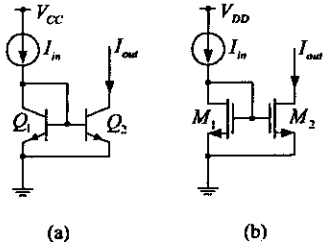

Figure 3. Simple current mirrors based on (a) BJT (b) MOS

2.4 A BiCMOS second generation current controlled current conveyor

Fig. 4 displays a class AB translinear loop, which is used as input section. The BJT translinear is used to achieve linear adjustability of intrinsic resistance. When all transistors are considered to be matched elements and working in saturation-mode. The following currents can be obtained [28].

$$I_1 = I_B e^{(V_w/V_T)} \quad (8)$$

and

$$I_2 = I_B e^{-(V_w/V_T)}. \quad (9)$$

Due to

$$I_x = I_1 - I_2. \quad (10)$$

Substituting Eqs. (8) and (9) into (10), it yields

$$I_x = 2I_B \sinh(V_{xy}/V_T). \quad (11)$$

Since $\sinh(V_{xy}/V_T) \cong V_{xy}/V_T$ for $V_{xy} \ll V_T$, we will obtain

$$R_x = \frac{V_T}{2I_B}. \quad (12)$$

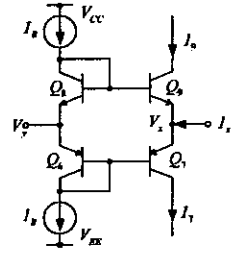

Figure 4. Class AB translinear loop

The BiCMOS class AB second generation current controlled current conveyor is shown in Fig. 5, which is modified from class A one in [29]. The circuit implementation consists of mixed translinear loops (Q_6-Q_9), which are DC biased by I_B. The z-terminal output that generates the current of x terminal is realized using transistors (M_4-M_5 and M_{12}-M_{13}). The x terminal resistance can be obtained by Eq. (12). From elementary small-signal circuit analysis, the output current I_Z of this circuit can be expressed as

$$I_z = \alpha I_x + \varepsilon, \quad (13)$$

where α and ε are current gain and offset error terms, respectively. By straightforward analysis of the circuit in Fig. 5 and $g_{mi} \gg g_{xi}$, we will obtain the α and ε as

$$\alpha = \frac{1}{g_{m4}g_{m12}}\left(\frac{g_{m4}g_{m9}g_{m13}}{g_{m9}+g_{m7}} + \frac{g_{m5}g_{m7}g_{m12}}{g_{m8}+g_{m7}}\right) \quad (14)$$

and

$$\varepsilon = K_1 + K_2, \quad (15)$$

where

$$K_1 = \frac{I_B}{g_{m4}g_{m8}g_{m12}}\left[\frac{g_{m4}g_{m7}g_{m9}g_{m13}}{g_{m9}+g_{m7}} + g_{m5}g_{m7}g_{m12}\left(\frac{g_{m7}}{g_{m8}+g_{m7}}\right.\right. \quad (16)$$

$$K_2 = \frac{I_B}{g_{m4}g_{m8}g_{m12}}\left[\frac{g_{m5}g_{m7}g_{m9}g_{m12}}{g_{m9}+g_{m7}} + g_{m4}g_{m8}g_{m13}\left(\frac{g_{m9}}{g_{m9}+g_{m7}}\right.\right. \quad (17)$$

If the transistors are matched, which means th $g_{m6} = g_{m7} = g_{m8} = g_{m9}$, $g_{m12} = g_{m13}$ a $g_{m4} = g_{m5}$, the current I_Z can be expressed as

$$I_z = I_x. \quad (18)$$

The output resistance looking into the z termir can be respectively expressed as

$$r_z \cong \frac{r_{ds}}{2}, \quad (19)$$

where r_{ds} is the drain-source resistance seen at t mentioned output terminal.

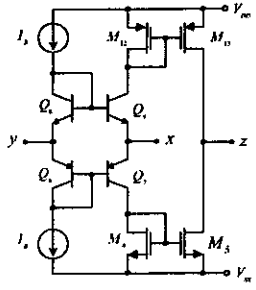

Figure 5. The BiCMOS class AB second-generat current controlled current conveyor

2.5 Modified BiCMOS Buffered Amplifier

Conventionally, the basic buffered amplifier can be realized by the circuit shown in Fig. 6(a consists of Q_{10}-Q_{12} and Q_{14p}, which is the translir loop. From elementary small-signal circuit analy

current, the proposed circuit can work as a current amplifier, while the magnitude of output current can be controlled by I_B and I_C. Furthermore, the output current is theoretically temperature-insensitive owing to no term of V_T.

For non-ideal case, the V_x, I_z and V_w of CC-CFA can be respectively characterized by

$$V_x = \beta V_y + I_x R_x,\ I_z = \alpha I_z + \varepsilon_z, \quad (34)$$

and

$$V_w = \gamma V_z + \varepsilon_b, \quad (35)$$

where α, β and γ are transferred error values deviated from one. ε_z and ε_b are the offset current and voltage at z, and w terminals, respectively. In the case of non-ideal and brief considerations, the I_O is subsequently changed to

$$I_O = \frac{I_A I_C}{I_B}\alpha_2\gamma_1\frac{\alpha_1}{1+\alpha_1} + \alpha_2\gamma_1\frac{I_C}{I_B}\frac{\varepsilon_{z1}}{1+\alpha_1} + \frac{\varepsilon_{b1}2I_C}{\alpha_2 V_T} + \varepsilon_{z2}. \quad (36)$$

From Eq. (36), we can see that the last three terms are offset currents. Consequently, to reduce the offset currents, the CC-CFA should be carefully designed to achieve these errors as low as possible. In addition, for the first term, these errors affect the magnitude of the output current. As a result, the magnitude output slightly depends on temperature due to temperature dependence of these errors. Thus, good design of the CC-CFA should be strictly considered to alleviate the effects.

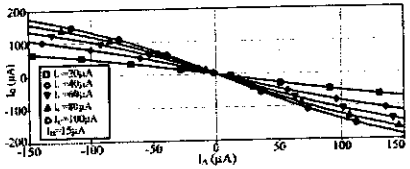

(a) Multiplication

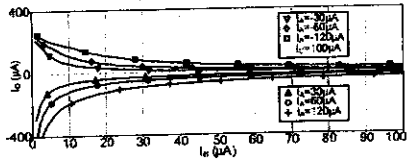

(b) Division

Figure 14. Static characteristics of the multiplier/divider in Fig. 13

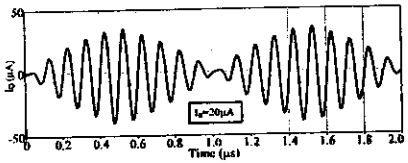

(a) Multiplication

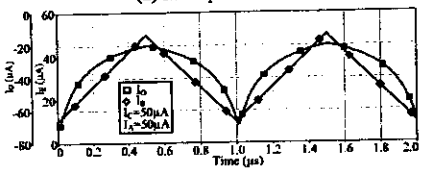

(b) Division

Figure 15. Transient responses of the multiplier/divider

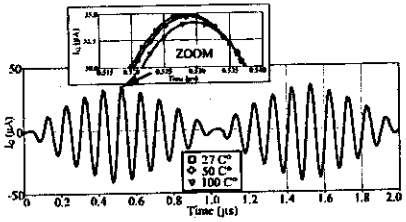

(a) Multiplication

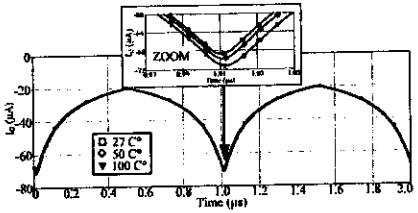

(b) Division

Figure 16. Output current deviations due to temperature variations of the multiplier/divider

Fig. 14(a) and (b) show the DC response characteristics of multiplication, where $I_B = 20\mu A$ and division of the proposed circuit, where $I_C = 100\mu A$, respectively.

Fig. 15(a) shows the transient responses of multiplication, where I_A and I_C were set to be a sinusoidal signal of $50\mu A_{P-P}$ at 10MHz and a triangular signal $50\mu A_P$ at 1MHz frequency, respectively. Fig. 15(b) shows the division of the proposed circuit, where I_A and I_C were set to be 50μA and I_B was a triangular signal with a frequency of 1MHz. Furthermore, the claimed temperature-insensitivities of the proposed circuit are confirmed by the results of Fig. 16, depicting transient responses.

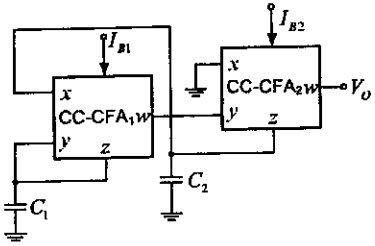

Figure 17. Oscillator based on the CC-CFA

6.2 Oscillator

The second application of proposed CC-CFA is an oscillator, shown in Fig. 17, which is modified from [35]. It consists of 2 CC-CFAs and 2 grounded capacitors. Considering the circuit in Fig. 17, and using the CC-CFA properties, yields the characteristic equation of this circuit as

$$s^2 C_1 C_2 R_{x1} R_{x2} + s(C_1 - C_2) + R_{x2} = 0. \quad (37)$$

From Eq. (37), it can seen that the proposed circuit can be set to be an oscillator if

$$C_1 = C_2. \quad (38)$$

Eq. (38) is called the condition of oscillation, thus the characteristic equation of the system becomes

$$s^2 + \frac{g_m}{C_1 C_2 R_x} = 0. \quad (39)$$

From Eq. (39), the oscillation frequency of this system can be obtained by

$$\omega_0 = \sqrt{\frac{1}{C_1 C_2 R_{x1} R_{x2}}}. \quad (40)$$

It can be seen that, from Eq. (40), the oscillation frequency (ω_0) can be controlled by the bias currents.

If non-ideal characteristics of the CC-CFA as explained in Eqs. (34) and (35) are considered and assuming that no offset current and voltage occur in the CC-CFA, the system characteristic equation can be written as

$$s^2 C_1 C_2 R_{x1} R_{x2} + s\left(C_1 - \alpha_1\beta_1 C_2\right) + \alpha_1\alpha_2\gamma_1\gamma_2\beta_2 = 0. \quad (41$$

In this case the oscillation condition and oscillation frequency are respectively changed to be

$$C_1 = \alpha_1\beta_1 C_2, \quad (42$$

and

$$\omega_0 = \sqrt{\frac{\alpha_1\alpha_2\gamma_1\gamma_2\beta_2}{C_1 C_2 R_{x1} R_{x2}}}. \quad (43$$

The confirmed performances of the oscillator can be seen in Fig. 18 and 19, showing the responses of the oscillator with bias currents, where I_{B1} and I_{B2} are equally set to 100μA. Fig. 20 shows the simulated output spectrum, where the total harmonic distortion (THD) is about 2.68%.

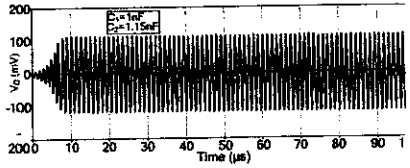

Figure 18. The simulation result of output waveform during initial state

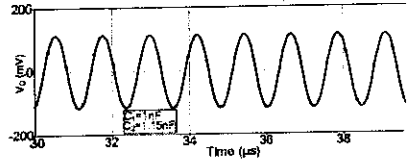

Figure 19. The simulation result of voltage waveform of oscillator in Fig. 17

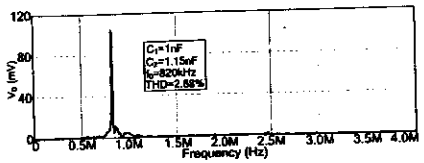

Figure 20. The simulation result of output spectrum

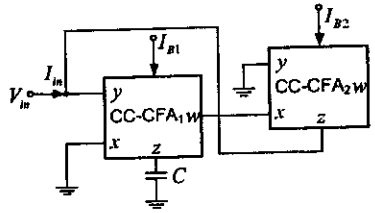

Figure 21. Grounded inductance simulator based on the CC-CFAs

6.3 Grounded inductance simulator

The grounded inductance simulator based on the CC-CFA is shown in Fig. 21, which is modified from [22], it employs 2 CC-CFAs and 1 grounded capacitor, which contrasts to ordinarily proposed circuits [36-37] in such that it consumes a few number of elements. From routine analysis and by using the CC-CFA properties, the input impedance of the circuit can be written as

$$Z_{in} = \frac{V_{in}}{I_{in}} = sCR_{z1}R_{z2}. \qquad (44)$$

From Eq. (44), it is obvious that the circuit shown in Fig. 21 performs a grounded inductance with a value

$$L_{eq} = CR_{z1}R_{z2} = \frac{CV_T^2}{4I_{B1}I_{B2}}. \qquad (45)$$

From Eq. (45), the inductance value L_{eq} can be adjusted electronically by either I_{B1} or I_{B2}.

If non-ideal characteristics of the CC-CFA as explained in Eqs. (34) and (35) are considered and assuming that no offset current and voltage occur in the CC-CFA, the input impedance can be written as

$$Z_{in} = \frac{sCR_{z1}R_{z2}}{\alpha_1\beta_1\gamma_1\alpha_2} = \frac{sCV_T^2}{\alpha_1\beta_1\gamma_1\alpha_2 4I_{B1}I_{B2}} \qquad (46)$$

From Eq. (46), for non-ideal consideration, these error parameters will effect to the inductance value. The impedance and phase of the simulator relative to frequency are also shown in Fig. 22, where $C=1nF$, $I_{B1}=I_{B2}=100\mu A$. Fig. 23 shows impedance values relative to frequency of the simulator for different I_B. To illustrate an application of the grounded inductance simulator, it is employed in an RLC parallel circuit shown in Fig. 24, where $I_{in} = 20\mu A$. The frequency responses of I_{LP}, I_{HP} and I_{BP} are shown in Fig. 25.

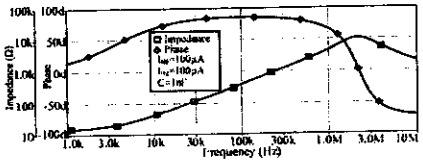

Figure 22. The impedance and phase relative to frequency of the grounded inductance simulator in Fig. 21

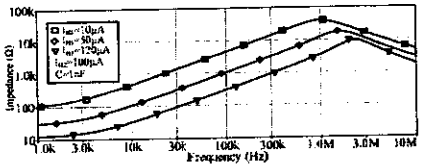

Figure 23. The impedance values relative to frequency of the simulators for different I_{B1}

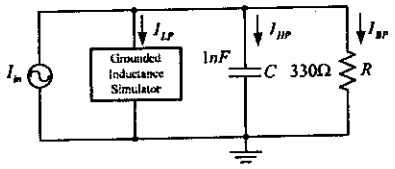

Figure 24. Parallels RLC resonant circuit

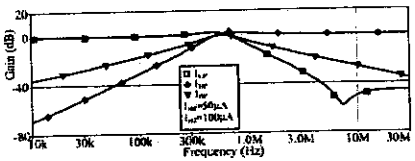

Figure 25. Simulated current characteristics of the resonant circuit in Fig. 24

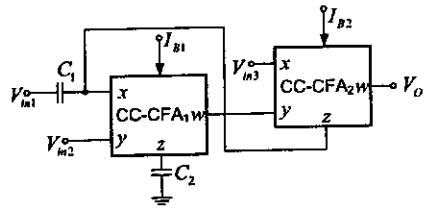

Figure 26. Voltage-mode universal biquad filter based on the CC-CFAs

6.4 Voltage-mode biquad filter

The voltage-mode biquad filter based on the CC-CFAs is shown in Fig. 26. By straightforward analysis of the circuit in Fig. 26, the output voltage of the network can be obtained as

$$V_O = \frac{V_{in1}s^2C_1C_2R_{z1}R_{z2} + V_{in2}(1+sC_2R_{z2}) - V_{in3}sC_2R_{z1}}{s^2C_1C_2R_{z1}R_{z2} + sC_2R_{z2} + 1}. \qquad (47)$$

From Eq. (47), the magnitudes of input voltages V_{in1}, V_{in2}, and V_{in3} are chosen as shown in Table. III to obtain a standard function of the 2nd order network. From Eq. (47), the pole frequency (ω_0) and quality factor (Q_0) of each filter response can be respectively expressed as

$$\omega_0 = \sqrt{\frac{1}{C_1C_2R_{z1}R_{z2}}}, \qquad (48)$$

and

$$Q_0 = \sqrt{\frac{C_1R_{z1}}{C_2R_{z2}}}. \qquad (49)$$

Substituting intrinsic resistance as depicted in Eq. (12), it yields

$$\omega_0 = \frac{2}{V_T}\sqrt{\frac{I_{B1}I_{B2}}{C_1C_2}}, \qquad (5$$

and

$$Q_0 = \sqrt{\frac{C_1I_{B2}}{C_2I_{B1}}}. \qquad (5$$

From Eqs. (50) and (51), by maintaining the rat I_{B1} and I_{B2} to be constant, it can be remarked th the pole frequency can be adjusted by I_{B1} and I without affecting the quality factor.

TABLE III

The V_{in1}, V_{in2} and V_{in3} values selection for each filter function response

Filter Responses		Input selections		
V_O		V_{in1}	V_{in2}	V_{in3}
BP		0	0	1
HP		1	0	0
BR	($R_{X1}=R_{X2}$)	1	1	1
AP	($R_{X1}=R_{X2}$)	1	1	2
LP	($R_{X1}=R_{X2}$)	0	1	1

If non-ideal characteristics of the CC-CFA explained in Eqs. (34) and (35) are considered a assuming that no offset current and voltage occur the CC-CFA, the output voltage can be written as

$$V_O = \frac{\gamma_2 s^2C_1C_2R_{z1}R_{z2}V_{in1} + (\beta_1\beta_2\gamma_1\gamma_2\alpha_1\alpha_2 + \beta_1\gamma_1 sC_2R_{z2})V_{in2}}{s^2C_1C_2R_{z1}R_{z2} + sC_2R_{z2} + \beta_2\gamma_1\alpha_1\alpha_2} \qquad (5$$

In this case, the ω_0 and Q_0 are changed to

$$\omega_0 = \sqrt{\frac{\alpha_1\alpha_2\beta_2\gamma_1}{C_1C_2R_{z1}R_{z2}}}, \qquad (5$$

and

$$Q_0 = \sqrt{\frac{\alpha_1\alpha_2\beta_2\gamma_1C_1R_{z1}}{C_2R_{z2}}}. \qquad (5$$

To prove the performances of the voltage-mo filter, the PSPICE simulation program was used the examination, where $I_{B1}=I_{B2}=50\mu A$ a $C_1=C_2=1nF$. The results shown in Fig. 27 are gain and phase responses of the voltage-mode fil obtained from Fig. 26. This clearly shows that circuit can provide low-pass, high-pass, band-pa band-rejcct, and all-pass functions depending digital selection [35] as shown in Table III, with modifying circuit topology. Fig. 28 shows g

responses of band-pass function where I_{B1} and I_{B2} are equally set to keep the ratio to be constant and changed for several values. It is found that pole frequency can be adjusted without affecting the quality factor, as earlier explained.

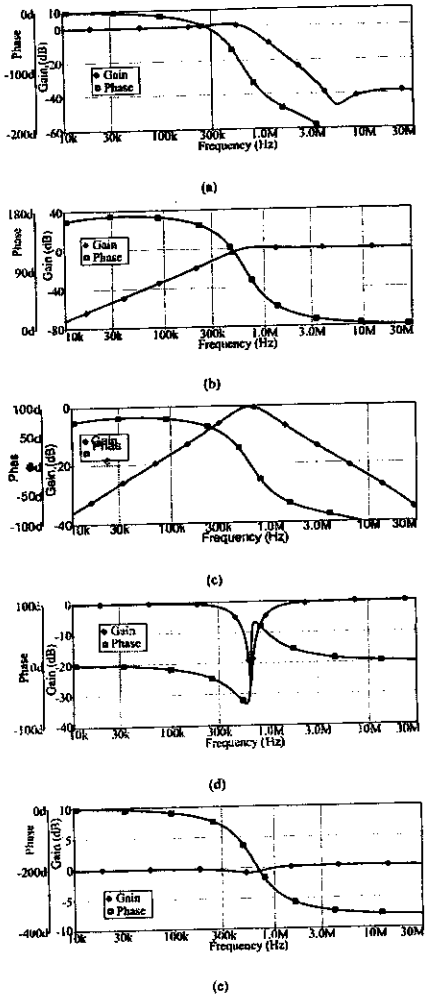

Figure 27. Gain and phase responses of the voltage-mode biquad filter in Fig. 24 for different responses (a) LP (b) HP (c) BP (d) BR (e) AP

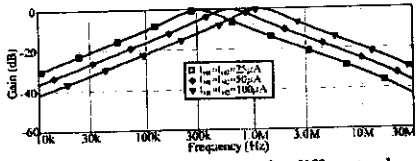

Figure 28. Band-pass responses for different values of I_{B1} and I_{B2} with keeping their ratios constant

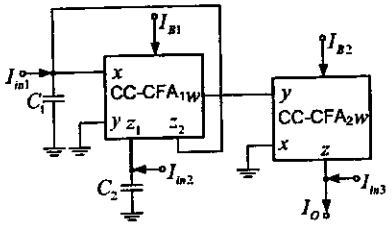

Figure 29. Current-mode universal biquad filter based on the CC-CFA

6.5 Current-mode biquad filter

The fifth application of the proposed CC-CFA is a current-mode biquad filter shown in Fig. 29. It employs only 2 active elements and 2 grounded capacitors, which is easy to fabricate, unlike the previous circuits [38-39]. The CC-CFA in Fig. 29 is slightly modified from the proposed CC-CFA in Fig. 7 by using multiple-output CC-CFA which can be achieved by using the current mirrors to copy current from the z_1 to the z_2 terminal to extend the usability of CC-CFA. Straightforward analysis of the circuit in Fig. 29 and using CC-CFA properties in section 2, the output current of the network can be obtained as

$$I_O = \frac{I_{in1}sC_1R_{x2} + I_{in2} - I_{in3}\left(s^2C_1C_2R_{x1}R_{x2} + sC_2R_{x2} + 1\right)}{s^2C_1C_2R_{x1}R_{x2} + sC_2R_{x2} + 1}. \quad (55)$$

TABLE IV

The I_{in1}, I_{in2} and I_{in3} value selections for each filter function response

Filter Responses	Input selections		
I_O	I_{in1}	I_{in2}	I_{in3}
BP	1	0	0
HP	1	1	1
BR	1	0	1
AP	2	0	1
LP	0	1	0

From Eq. (55), the magnitudes of input currents I_{in1}, I_{in2}, and I_{in3} can be chosen as in Table. IV to obtain a standard function of the 2nd order network. The circuit for selection can be seen in [40]. Moreover, I_{in1} must be double of I_{in3} in the case of AP. So to achieve this condition, the current amplifier which has gain of 2 is required. From Eq. (55), the pole frequency (ω_0) and quality factor (Q_0) of each filter response can be respectively expressed as

$$\omega_0 = \sqrt{\frac{1}{C_1C_2R_{x1}R_{x2}}}, \quad (56)$$

and

$$Q_0 = \sqrt{\frac{C_1R_{x1}}{C_2R_{x2}}}. \quad (57)$$

Substituting intrinsic resistance as depicted in Eq. (12), it yields

$$\omega_0 = \frac{2}{V_T}\sqrt{\frac{I_{B1}I_{B2}}{C_1C_2}}, \quad (58)$$

and

$$Q_0 = \sqrt{\frac{C_1I_{B2}}{C_2I_{B1}}}. \quad (59)$$

If non-ideal characteristics of the CC-CFA as explained in Eqs. (34) and (35) are considered and assuming that no offset current and voltage occur in the CC-CFA, the output current in Fig. 29 can be written as

$$I_O = \frac{I_{in1}sC_2R_{x2}\alpha_{12} + I_{in2}\alpha_2\beta_2\gamma_1\alpha_{12} - I_{in3}D(s)}{D(s)}, \quad (60)$$

where $D(s) = s^2C_1C_2R_{x1}R_{x2} + sC_2R_{x2} + \beta_2\gamma_1\alpha_{11}\alpha_{12}\alpha_2$.
In this case, the ω_0 and Q_0 are changed to

$$\omega_0 = \sqrt{\frac{\beta_2\gamma_1\alpha_{11}\alpha_{12}\alpha_2}{C_1C_2R_{x1}R_{x2}}}, \quad (61)$$

and

$$Q_0 = \sqrt{\frac{\beta_2\gamma_1\alpha_{11}\alpha_{12}\alpha_2C_1R_{x1}}{C_2R_{x2}}}. \quad (62)$$

To prove the performances of the current-mode filter, the PSPICE simulation program was used with same conditions to the voltage-mode filter, where $I_{B1}=I_{B2}=100\mu A$ and $C_1=C_2=1nF$. The results shown in Fig. 30 are the gain and phase responses of the current-mode filter obtained from Fig. 29. This clearly shows that the circuit can provide low-pass, high-pass, band-pass, band-reject, and all-pass functions depending on digital selection as shown in Table IV, without modifying circuit topology. Fig. 31 shows gain responses of band-pass function where I_{B1} and I_{B2} are equally set to keep the ratio to be constant and changed for several values. It is found that pole frequency can be adjusted without affecting the quality factor.

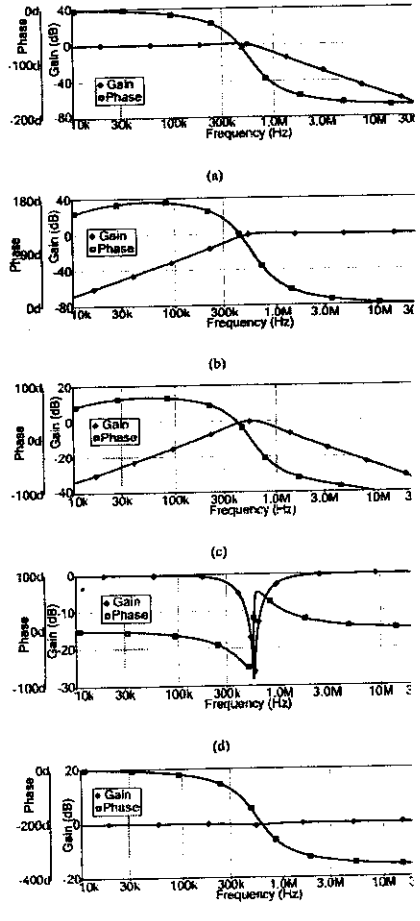

Figure 30. Gain and phase responses of the current-mode biquad filter in Fig. 29 for different responses (a) LP (b) HP (c) BP (d) BR (e) AP

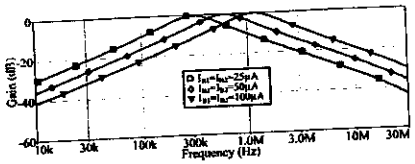

Figure 31. Band-pass responses for different values of I_{B1} and I_{B2} with keeping their ratios constant

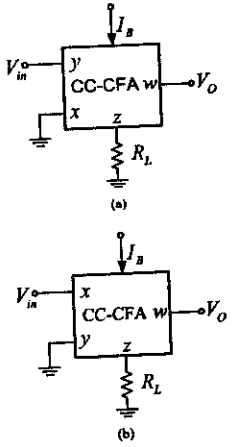

Figure 32. (a) Inverting Amplifier (b) Non-Inverting Amplifier

6.6 Voltage Amplifiers

The voltage non-inverting and inverting amplifiers based on the CC-CFA are shown in Fig. 32(a) and (b), respectively. By straightforward analysis of the circuit in Fig. 32, the output voltages of the circuits can be respectively obtained as

$$V_O = \frac{R_L}{R_x} V_{in}, \tag{63}$$

and

$$V_O = -\frac{R_L}{R_x} V_{in}. \tag{64}$$

Substituting intrinsic resistance, as depicted in Eq. (12), it yields

$$V_O = \frac{2I_B R_L}{V_T} V_{in}, \tag{65}$$

for non-inverting configuration and

$$V_O = -\frac{2I_B R_L}{V_T} V_{in}, \tag{66}$$

for inverting configuration. It can be seen from Eqs. (65) and (66) that the circuits in Fig. 32(a) and (b) can perform as voltage amplifiers whose voltage gain can be electronically controlled via control current I_B.

If non-ideal characteristics of the CC-CFA as explained in Eqs. (34) and (35) are considered, the output voltages can be rewritten as

$$V_O = \alpha\beta\gamma R_L \frac{V_{in}}{R_x} + \gamma R_L \varepsilon_z + \varepsilon_b, \tag{67}$$

for non-inverting configuration and

$$V_O = -\left(\alpha\gamma R_L \frac{V_{in}}{R_x} + \gamma R_L \varepsilon_z + \varepsilon_b\right), \tag{68}$$

for inverting configuration, the last two terms of Eqs. (67) and (68) are offset voltages. Consequently, to reduce the offset voltages, the CC-CFA should be carefully designed to achieve these errors as low as possible. In addition, for the first term, these errors affect the magnitude of the output voltage.

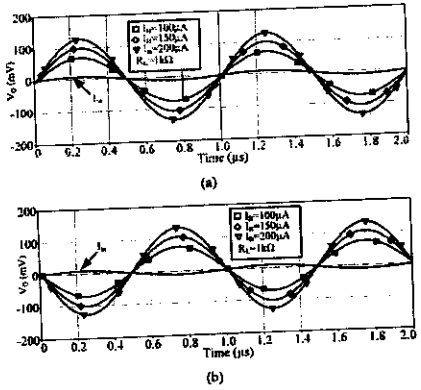

Figure 33. Output voltages relative to input bias current (a) non-inverting amplifier (b) inverting amplifier

Fig. 33(a) and (b) display the output voltages as a function of the input bias current I_B whereas V_{in}=10mV. These figures prove that the magnitude of the output voltage can be easily/electronically

controlled in accordance with the theoretical anticipations, as depicted in Eqs. (65) and (66).

7 Conclusion

The modified version of building block, called CC-CFA, has been introduced via this paper. The realization has been done by a BiCMOS technology to reduce offset errors at the outputs. The usabilities have been proven by the simulation and application examples. They consume a few numbers of components, while electronic controllability is still available, which differs from other recently proposed elements. The proposed CC-CFA provides low distortions, low output offset errors and wide bandwidth of frequency responses. It is very appropriate to realize in commercially-purposed integrated circuit for employing in instrumentation/measurement systems, battery-powered, portable electronic equipments or wireless communication systems. Our future work is to find more applications of the CC-CFA, emphasizing on the current or voltage-mode signal processing circuits such as signal generator, rectifier, etc.

Acknowledgement

This work was supported in part by a grant from King Mongkut's University of Technology North Bangkok (KMUTNB).

References:

[1] C. Toumazou, F. J. Lidgey, and D. G. Haigh, *Analogue IC design: the current-mode approach*, London: Peter Peregrinus, 1990.

[2] D. R. Bhaskar, V. K. Sharma, M. Monis and S. M. I. Rizvi, "New curren-mode universal biquad filter," *Microelectronics Journal*, vol. 30, pp. 837-839, 1999.

[3] A. Sedra and K. C. Smith, "A second-generation current conveyor and its applications," *IEEE Transactions on Circuits Theory*, vol. 17, pp. 132–134, 1970

[4] C. Acar and S. Ozoguz, "A new versatile building block: current differencing buffered amplifier suitable for analog signal processing filters," *Microelectronics Journal*, vol. 30, pp. 157–160, 1999.

[5] D. Biolek, "CDTA–Building Block for Current-Mode Analog Signal Processing," *Proceedings of the European conference on circuit theory and design 2003 - ECCTD'03*, Krakow, Poland, pp. 397–400, 2003.

[6] Comlinear Corp., "Designer's guide for 20(series op amp," *Application note 200-1*, 480(Wheaton Drive, Ft. Collins, CO 80525, 1984.

[7] Analog Devices: "Linear products data book.' Norwood MA, 1990.

[8] A. Fabre, "Insensitive voltage mode an current mode filters from commercially available transimpedance opamps," *Proc. IE (G)*, vol. 140, pp. 319–321, 1993.

[9] S.-I. Liu and Y.-S. Hwang, "Realization of R-L and C–D impedances using a current feedback amplifier and its applications, *Electronics Letters*, vol. 30, no. 5, pp. 380 381, 1994.

[10] C.-M. Chang, C.-S. Hwang, and S.-H. Tu "Voltage-mode notch, lowpass and bandpas filter using current-feedback amplifiers, *Electronics Letters*, vol. 30, no. 24, pp. 2022 2023, 1994.

[11] M. T. Abuelma'atti and S. M. Al-shahran "New universal filter using two curren feedback amplifiers," *International Journal Electronics*, vol. 80, pp. 753–756, 1996.

[12] J-W. Horng and M-H. Lee,, "High inpu impedance voltage-mode lowpass, bandpas and highpass filter using current-feedbac amplifiers,". *Electronics Letters*, vol. 33, n 11, pp. 947–948, 1997.

[13] N. A. Shah nad M. A. Malil "Voltage/current-mode universal filter usin FTFN and CFA," *Analog integrated circui and signal processing*, vol. 45, pp. 197-20 2005.

[14] S. Selvanayagam and F.J. Lidgey, "Wi bandwidth CMOS current feedback op an for inverting amplifier applications," *I Colloquium, Modelling and Techniqu Wideband Circuits*, pp. 7/1-7/4, 1996.

[15] S. I. Liu, C. C. Chang, and D. S. Wu, "Activ R sinusoidal oscillators using CFOA pol *International Journal of Electronics*, vol. pp. 1035–1042, 1994.

[16] D. S. Wu, S. I. Liu, Y. S. Hwang, and Y. Wu, "Multiphase sinusoidal oscillator usi CFOA pole," *IEE Proc., Circuits, Devi Systems*, vol.142, pp. 37–40, 1995.

[17] M. T. Abuelma'atti and S. M. Al-Shahrani, novel low-component count single-eleme controlled oscillator using CFOA pol *International Journal of Electronics*, vol. pp. 747–753, 1996.

[18] R. Senani and V. K. Singh, "Novel sin resistance controlled oscillator configurati using current feedback amplifiers," *IE.*

Trans. Circuits Syst. I, vol. 43, pp. 698–700, 1996.

[19] S. S. Gupta, D. R. Bhaskar, R. Senani, "New voltage controlled oscillators using CFOAs," *International Journal of Electronics and Communications*, available online, 2008.

[20] S. Natarajan, "Inductance simulation using modern current feedback amplifiers (CFAs)," *Proceedings of the Thirty-Seventh Southeastern Symposium on System Theory, 2005, SSST'05,*, pp. 60-64, 2005.

[21] T. K. Bandyopadhyay, R. K. Nagaria,S. K. Sanyal and R. Nandi, "Lossless inductor using current feedback amplifier," *International Symposium on Signals, Circuits and Systems, 2005. ISSCS 2005*, vol. 2, pp. 689-692, 2005.

[22] A. Fabre, "Gyrator implementation from commercially available transimpedance operational amplifiers," *Electronics Letters*, vol. 28, pp. 263-264, 1992.

[23] M. Abuelma'atti and S. al-Shahrani, "New CFOA-based triangular/square wave generator," *International Journal of Electronics*, vol. 84, pp. 583–588, 1998.

[24] M. Weng, J. R Lai and M. H. Lee, "Realization of. nth-order series impedance function using only (n-1). current-feedback amplifiers,". *International Journal of Electronics*, vol. 87, no. 1, p. 63-69, 2000.

[25] H. Z. Abouda and A. Fabre, "New high-value floating controlled resistor in CMOS technology," *IEEE Transaction on Instrumentation and Measurement*, vol. 51, no. 7, pp.1017-1020, 2006.

[26] M. Siripruchyanun and W. Jaikla, "Electronically Controllable Current-Mode Universal Biquad Filter Using Single DO-CCCDTA," *Circuits Systems and Signal Processing*, vol. 27, pp. 113-122, 2008.

[27] P. R. Gray, P. J. Hurst S. H. Lewis and R. G. Meyer, *Analysis and Design of Analog Integrated Circuits*, New York: John Wiley & Sons, 2001.

[28] A. Fabre, "Dual translinear voltage/current convertor," *Electronics Letters*, vol. 19, pp. 1030-1031, 1983.

[29] F. Seguin and A. Fabre, "2 GHz controlled current conveyor in standard 0.8μm BICMOS technology," *Electronics Letters*, vol. 37, pp. 329-330, 2001.

[30] H. Barthélemy and E. Kussener, "High speed voltage follower for standard BiCMOS technology," *IEEE Transaction on Circuits and Systems*, vol. 48, pp. 727-732, 2001.

[31] A. Grebene, *Bipolar and MOS analog integrated circuit design*, John Wiley & Sons, Inc., New York, 1984.

[32] D. R. Frey "Log-domain filtering: an approach to current-mode filtering," *IEE Proc. Circuit Devices Syst.*, vol. 140. pp. 406-416, 1993.

[33] E. Yuce, S. Tokat, A. Kızılkaya and O. Cicekoglu, "CCII-based PID controllers employing grounded passive components," *International Journal of Electronics and Communication*, vol. 60, no. 5, pp. 399-403, 2006.

[34] M. T. Abuelma'atti and M.A. Al Qahtani, "A current mode current controlled current conveyor based analogue multiplier/divider," *International Journal of Electronics*, vol. 85, pp. 71-77, 1998.

[35] D. R. Bhaskar and Raj Senani, "New CFOA-Based single-element-controlled sinusoidal oscillators," *IEEE Transaction on Instrument and Measurement*, vol. 55, pp. 2004-2221, 2006.

[36] I. A. Khan and M. H. Zaidi, "A novel ideal floating inductor using translinear conveyors," *Active and Passive Electronic Components*, vol. 26, no. 2, pp. 87–89, 2003.

[37] J. S. Pena-Finol and J. A. Connelly, "Novel lossless floating immittance simulator employing only two FTFNs," *Analog Integrated Circuits and Signal Processing*, vol. 29, no. 3, pp. 233-235, 2001.

[38] W. Tangsrirat, "Low-voltage digitally programmable current-mode universal biquadratic filter," *International Journal of Electronics and Communication*, vol. 62, pp. 97-103, 2008.

[39] M. A. Ibrahim, S. Minaei, and H. A. Kuntman "A 22.5 MHz current-mode KHN-biquad using differential voltage current conveyor and grounded passive elements," *International Journal of Electronics and Communication*, vol. 59, pp. 311-318, 2005.

[40] C. L. Hou, C. C. Huang, Y. S. Lan, J. J. Shaw and C. M. Chang "Current-mode and voltage-mode universal biquads using a single current-feedback amplifier," *International Journal of Electronics*, vol. 86, no. 8, pp. 929-932, 1999.